Magnesium Technology 2012
Edited by: Suveen N. Mathaudhu, Wim H. Sillekens, Neale R. Neelameggham, and Norbert Hort
TMS (The Minerals, Metals & Materials Society), 2012

MECHANICAL AND CORROSION PROPERTIES OF AS-CAST AND EXTRUDED MG10GD ALLOY FOR BIOMEDICAL APPLICATION

Petra Maier[1], Sören Müller[2], Hajo Dieringa[3], Norbert Hort[3]
[1]University of Applied Scienes Stralsund, Zur Schwedenschanze 15, D-18435 Stralsund, Germany
[2]Extrusion Research and Development Center TU Berlin, Gustav-Meyer-Allee 25, D-13355 Berlin, Germany
[3]Helmholtz-Zentrum Geesthacht, Magnesium Innovation Center, Max-Planck-Straße 1, D-21502 Geesthacht, Germany

Keywords: Magnesium Rare-Earth Alloys, Extrusion, Fatigue, Corrosion, Biomedical Application

Abstract

Due to the good specific strength and the moderate corrosion rate Mg-RE alloys have found growing interest for medical applications as implant material. In this study extruded Mg10Gd has been investigated, once by potentiodynamic method and again under cyclic load. Corrosion exposure is known to reduce the fatigue strength strongly. The data are compared to Mg10Gd as-cast condition and show an increase in fatigue properties and similar corrosion behavior. The form of corrosion and the influence of the temperature during voltammetric tests are discussed. A temperature increase from room to body temperature accelerates the corrosion processes. Due to stress peaks under load pitting corrosion is not preferred. The influence of the microstructure on the corrosion form is discussed. Casted Mg10Gd reveals large dendrites, which change into a globular microstructure during extrusion resulting in improved mechanical properties, mostly the elongation to fracture up to 20 %.

Introduction

The fact that Magnesium corrodes with time is an advantage in biodegradable material applications. Magnesium has a standard reduction potential of -2.37 Volts and this makes it to be preferentially degraded when in contact with other metals in an aqueous environment [1]. For structural application, this material property is completely abhorred and efforts are made to control the corrosion processes by all means [2,3,4]. However, this is different with biodegradable material for human implantation purposes such as bones or stents [5,6,7,8]. For these applications, permanent retention of implanted materials in the body is considered unnecessary after the healing processes are completed. This leads to the idea of material degradation with time in the body. Different types of materials have been proposed for use in this area taking cognisance of their biocompatibility and corrosion properties. These include Magnesium and its alloys [9,10], pure iron with Manganese [11,12] and polymers especially the so called self expansible poly-l-lactic acid (PLLA) and poly-l-glycolic acid (PLGA) origin [13,14]. Results of some of the past investigations on biodegradable materials for bone or cardio-vascular application are summarised elsewhere [7,15]. Magnesium alloys show very promising results for both bone regeneration and cardio-vascular application purposes, however there are also challenges [9]. Candidate materials should be able to compromise between mechanical properties and material degradation during implantation period. Very fast degradation rate will lead to restenosis or thrombosis in the case of stents for vascular application [7,16] as a result of the early loss of the load bearing capacity of the stents. For bone support and regeneration, that could lead to excessive gas formation, irritation, fracture or complication on the unhealed bones and the surrounding tissues [9]. Since the behavior of the implant materials are not dependent on the materials alone but also on the implant environment, in vitro and in vivo experiments are essential for material screenings and clinical trials respectively [17]. Several factors play a role in determining the final material properties. These include material purity, alloying elements, processing route and post processing operations. Recent work shows that alloying pure Magnesium with Gadolinium improves its mechanical and corrosion properties [18]. However, little is known about the corrosion fatigue of these potential implant alloys. In order to explore this further, forming by extrusion in comparison to the as-cast condition has been adopted to control the microstructure and improve the mechanical properties under supervision of the corrosion behavior. Consequently their cyclic behavior and corrosion fatigue properties were investigated. This work summarises the preliminary results of the microstructure, corrosion response, fatigue and corrosion fatigue behaviors of the extruded alloy in comparison to the as-cast condition. Furthermore the temperature during the corrosion tests has been increased from room to body temperature (37 °C).

Materials and Experimental

Fatigue and corrosion fatigue tests were carried out on extruded Mg10Gd produced at the Extrusion Research and Development Center TU Berlin. The materials (bars) were directly extruded at an overall temperature of 420 °C, an extrusion speed of 1 mm/s and a deformation degree φ of 1.6 ($\varphi = \ln A_1/A_0$). Before extrusion the material was casted by permanent mould direct chill casting at Helmholtz Centre Geesthacht. Detailed information on the casting process is given in [19]. The microstructure during extrusion has changed dramatically. The obtained optical micrographs from the as-cast permanent mould chill cast show mainly coarse and columnar structures (up to 500 µm), see figure 1. These columnar grains were characterized by dendrite arms according to the preferred orientation during solidification process.

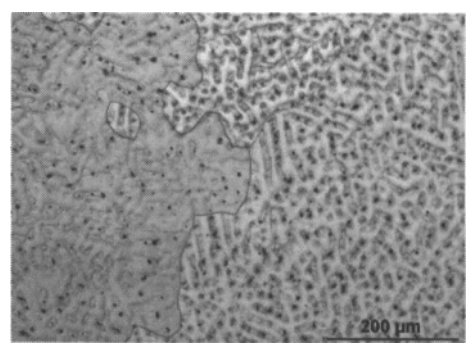

Figure 1. Microstructure of Mg10Gd, as-cast, permanent mould direct chill casting

Figure 2 presents grain refinement of the extruded material with an average grain size of 15 µm. The formations of the black lines, which will consist of aligned second phases, indicate the extrusion direction. The influence of this alignment is part of this study.

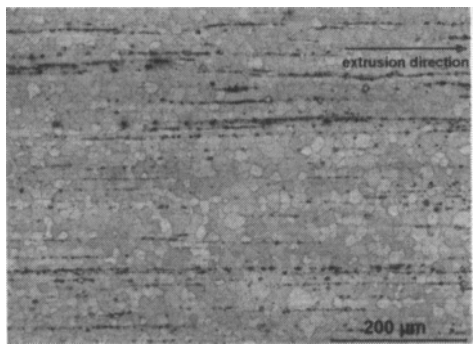

Figure 2. Microstructure Mg10Gd, extruded, extrusion temperature 420 °C, extrusion speed of 1 mm/s, deformation degree φ of 1.6

To evaluate the stress amplitude of the fatigue tests tensile and compression tests were carried out according to EN 10002-1:2001 standard. Tensile stress-strain curves of the extruded material are shown in figure 3 and compression stress-strain curves in figure 4, respectively. The mechanical properties of the extruded material in comparison to the as-cast condition [20] are summarized in table I. A Young's modulus of 42.9 GPa was additionally evaluated from the tensile tests, but not shown in table I. Due to the hexagonal crystal an anisotropic behavior in the elastic moduli (Young's and bulk modulus) occurs, which is a well known fact.

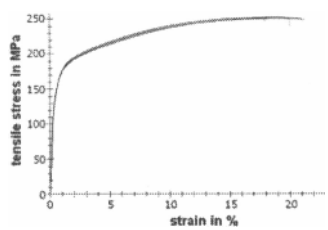

Figure 3. Tensile stress-strain curves of extruded Mg10Gd

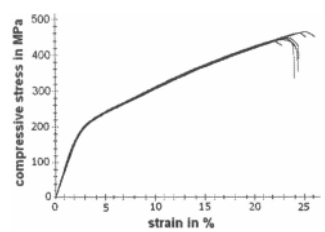

Figure 4. Compression stress-strain curves of extruded Mg10Gd

From table I a strong increase of mechanical properties of the extruded material can be seen. Especially, the elongation to fracture (A) improved from not even 2 % to almost 20 %. The tensile-compressive yield asymmetry in wrought magnesium alloys (different value for tensile yield stress (TYS) and compression yield stress (CYS)) is known for magnesium alloys. The compressive yield stresses in wrought magnesium alloys has been previously found to the 0.6-0.7 times those of the tensile [21]. Such an asymmetric yield behavior, resulting in a poor compressive yield stress, would prohibit the potential application for these wrought Magnesium alloys as implant material being mostly exposed to compression load. However, for the Mg10Gd alloy the ratio of CYS/TYS is above 1 in longitudinal direction, which means that alloying with rare earth elements shows higher compression strength. This behavior might change in other directions. The influence of this asymmetrical plastic deformation behavior on the fatigue properties of wrought magnesium alloys have already been reported in [22, 23], also showing higher compression yield stress values of magnesium alloys alloyed with rare earth elements: cerium, neodymium and lanthanum.

Table I. Mechanical properties of Mg10Gd in different conditions

	TYS (MPa)	UTS (MPa)	A (%)	CYS (MPa)	ratio CYS/TYS
as-cast	60	91	1.78	76	1.26
extruded	148	251	19.42	176	1.19

Round samples (diameter of 6 mm) were machined with surface roughness of 6.3 µm, according to ISO 1099:2006. Fatigue and corrosion fatigue tests were performed on a closed-loop servo hydraulic testing machine system MTS820. Tests were carried out in stress controlled mode using constant load with a stress ratio of R = -1 and a frequency of 5 Hz. These parameters allow comparison to data given in the literature, even being aware that implants are mostly exposed to compression load, however they are still a dynamic system. Measurements were limited to $2*10^6$ cycles while Ringer-Acetate solution was used as the corrosive media in the corrosion fatigue test. A voltammetric cell (measurement area of 150 mm²) was used to evaluate the free corrosion potential (Open Circuit Potential -OCP-) and passivity. The OCP and the current density - potential curve were measured using an Argenthal reference electrode. The microstructure and fracture surfaces of the investigated alloys were characterized using a Zeiss EVO 40XVP Scanning Electron Microscope (SEM) equipped with an Energy Dispersive X-ray Spectroscopy (EDX) for chemical analysis.

Fatigue test results

Fatigue tests on as-cast Mg10Gd as evaluated shows fatigue strength (failure probability of 50 percent) of 52 MPa [20]. During fatigue tests, the cyclic deformation behavior of the alloys was monitored by evaluating the movement (cyclic creep) and change in shape (material strengthening / softening) of the hysteresis loop based on the number of cycles. Figure 5 represents the cyclic creep behavior subjected to 50 MPa stress resulting at $1.8*10^6$ cycles to fracture. Due to asymmetrical plastic deformation in the tensile and compressive half cycle, the specimen exhibit pronounced cyclic tensile creep in the second half of the life time.

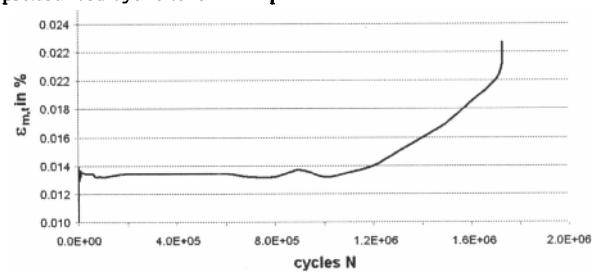

Figure 5. Cyclic creep curves of as-cast Mg10Gd at 50 MPa

The fatigue strength value of the extruded Mg10Gd alloy has not been evaluated yet. However, first fatigue tests have been done to investigate the cyclic creep behavior. According to the higher mechanical properties of the tensile and compression tests of extruded Mg10Gd a stress amplitude of 120 MPa has been chosen. This stress amplitude is higher than the UTS value for the as-cast material. Figure 6 presents the cyclic creep behavior of the extruded material. Extrusion processing has slightly decreased the asymmetric yield behavior (see ratio of CYS/TYS in table I), but the value is still above one. Thus the resistance to plastic deformation is, similar to the as-cast condition, stronger in the second half of the cycle and lead to cyclic tensile creep. However, after $1*10^6$ cycles cyclic creep changes into compressive creep and saturates; hardening effects are expected to appear.

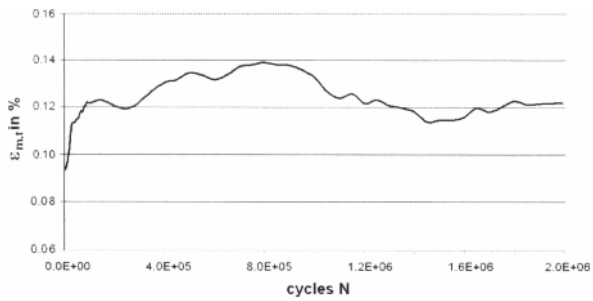

Figure 6. Cyclic creep curve of extruded Mg10Gd at 120 MPa

According to the higher strength and elongation to fracture values of the extruded material and the exposure to a higher stress amplitude the total mean strain ($\varepsilon_{m,t}$) shows higher overall values.

Figure 7 shows the SEM fracture surfaces of the as-cast alloy, loaded at a stress amplitude of 50 MPa, and figure 8 the extruded alloy, loaded at 150 MPa ($2*10^4$ cycles), respectively. The as-cast fracture surface is generally brittle in nature, explained by the low elongation to fracture value due to the coarse grained microstructure (less than 2 %). However, the characteristic fracture surface of fatigue failure has been seen. Due to the brittle behavior more than one crack initiation have been found leading via the area with fatigue striations (growth bands) into the final rupture area, which often shows strong crystal oriented fatigue structures, also seen in other castings [24].

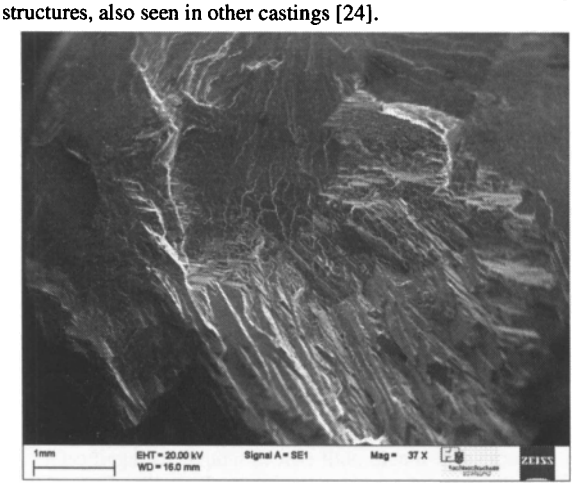

Figure 7. SEM micrograph of fracture surface: as-cast; 50 MPa

The extruded fracture surface indicates a more ductile damage and fracture behavior, which was expected because of the elongation to fracture of almost 20 %. There are no crystal oriented fatigue structures. SEM fractography with higher magnification show spherical dimples, which are characteristic of ductile fracture.

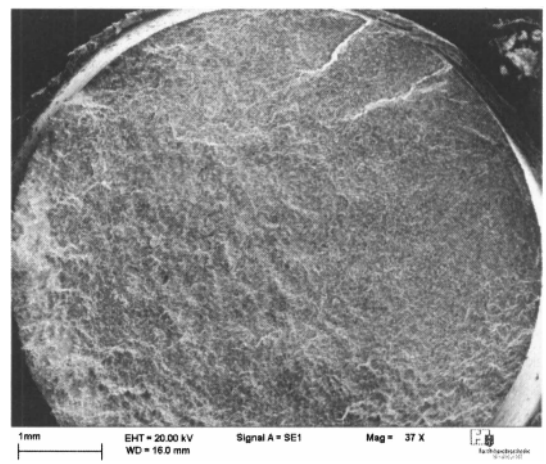

Figure 8. SEM micrograph of fracture surface: extruded, 150 MPa

Voltammetric measurement results

The corrosion behavior of the alloys in Ringer-Acetate solution has been evaluated by potentiondynamic measurements using an electrolytic cell. The exposed area of ~ 150 mm² is orientated transversely to the extrusion direction. Figure 9 shows the OCP measurement of the as-cast condition in dependence of the temperature. As-cast Mg10Gd reaches its free potential of -1700 mV at 37 °C already after 150 sec. The OCP value shifts towards noble potential as a result of passivation. However, as-cast Mg10Gd at 20 °C reaches saturation (defined by no change in potential values) after 500 sec, more slowly and the OCP value shows a slight lower free potential of -1690 mV (more noble).

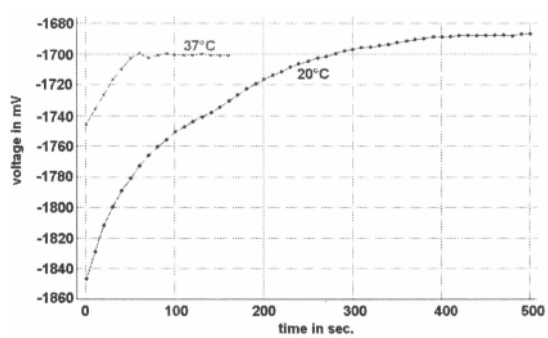

Figure 9. OCP measurements of Mg10Gd at 20°C and 37°C: as-cast

The influence of the grain refinement during extrusion on corrosion of the extruded material is seen in figure 10. The OCP value of the corrosion test at 37 °C is reached after 150 sec, almost unchanged compared to the casting. At 20 °C saturation of the wrought material is reached earlier compared to the casting, after 210 sec, showing more negative free potential.

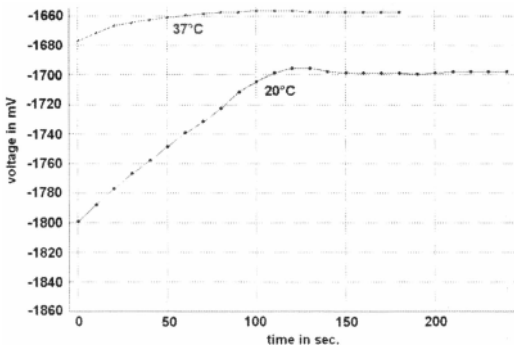

Figure 10. OCP measurements of Mg10Gd at 20°C and 37°C: extruded

The current density - voltage curves in figure 11 (i-E curves) show the difference of corrosion behavior (concentrated on the anodic reaction) in dependence of the temperature of as-cast material, figure 12 of wrought material, respectively. The free potential, passivation and breakthrough values seem not to be influenced strongly. However, increasing the voltage after breakthrough data of current density show an influence of temperature. Increasing the temperature to 37 °C accelerates the corrosion process, for the as-cast as well the wrought alloy. After strong anodic corrosion, passivation starts again. However, the passive layer is not stable by increasing voltage (growth and dissolution can be seen). At high voltage values the influence of the temperature on the corrosion behavior is almost eliminated.

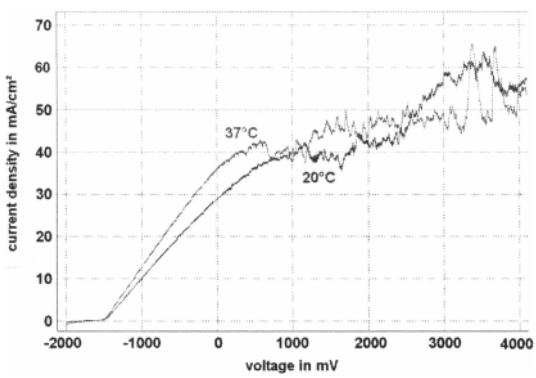

Figure 11. Potentiodynamic measurements (i-E curves) of Mg10Gd at 20 °C and 37 °C: as-cast

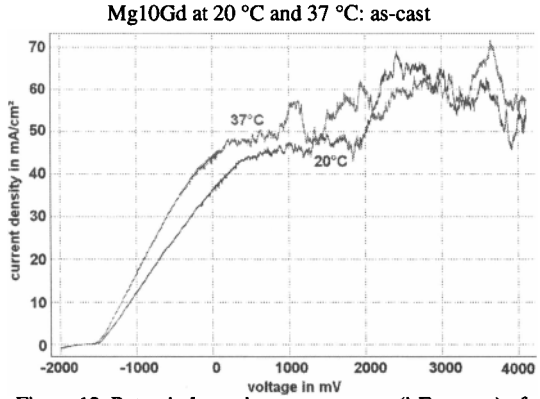

Figure 12. Potentiodynamic measurements (i-E curves) of Mg10Gd at 20 °C and 37 °C: extruded

Microscopic investigations of the corroded material are planned to evaluate the microstructural influence of aligned second phases. The corrosion process is expected to start at areas where high differences in potential occur, but so far the potential value of the precipitate Mg_5Gd is not known yet. However, precipitates are expected to be nobler than the matrix itself.

Corrosion fatigue results

Corrosion fatigue tests show that the numbers of cycles to fracture are reduced considerably due to Ringer-Acetate solution. Again, extruded Mg10Gd sustained higher cycles to fracture than as-cast Mg10Gd in corrosive medium, obviously depending on the stress amplitude. For stresses of 120 MPa extruded Mg10Gd fractured after 600000 cycles; without the exposure to the electrolyte the samples reached the limited $2*10^6$ cycles, see table II.

Table II. Comparison in fatigue life: without and with exposure to the electrolyte (Ringer-Acetate solution), at 20 °C

material	cycles, without	cycles, with
as-cast (50 MPa)	$> 1.8*10^6$	26,000
extruded (120 MPa)	$> 2*10^6$ (limited value)	600,000

Figure 13 (a, b) shows the development of selective corrosion on the surface of the sample in the fatigue corrosion chamber while figure 13 (c) shows the fractured sample with corrosion products.

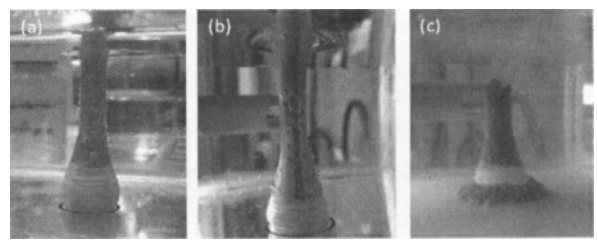

Figure 13. Different stages during fatigue corrosion test (a) hydrogen evolution (b) selective corrosion (c) fractured sample with corrosion products

To find out if the selective corrosion is developing into corrosion pitting further investigations need to be done. First light microstructural images of the as-cast and wrought material (cross sections have been looked at) have shown rather homogenous corrosion behavior, which will be preferred for medical implants.

Discussion

Microstructure

From initial thermodynamic calculations using Pandat software for Mg-Gd binary system [25], HCP and Mg_5Gd precipitates were predicted. The formation of Mg_5Gd is possible at the eutectic temperature of 548 °C with a maximum solubility of 23.49 wt. % [26]. This phase has been observed in previous work and is known to be effective in improving the mechanical property of pure Magnesium [18]. From the two alloys investigated, extruded material shows strongly refined grain size followed by strongly improved mechanical properties. This binary phase will later play a role on the fatigue and corrosion fatigue response of the investigated alloys. The coarse nature of the as-cast grains (>500 µm) of permanent mould chill cast techniques is significantly a weakness to its mechanical properties as this will influence the

efficacy of the precipitates potency to opposing dislocation movement. Extrusion at the high deformation degree of 1.6 requires high temperatures (420 °C). The grain refinement as a result of recrystallization improves strength and ductility due to grain size strengthening. However, the uniformly distributed precipitates form lines in extrusion direction. As observed from the EDX analysis results of the casted alloy, it is clearly seen that there are lower amount of rare earth elements dissolved in the solid solution. This phenomenon is known to be associated with oxidation of the rare earth elements during casting. Rare earth elements form oxides that are heavier than the Magnesium melt and in most cases exist as inclusions on the cast material or are removed during casting [18, 27, 28]. During heat exposure of the extrusion process enough energy is given for further diffusion processes between Mg_5Gd precipitates and solid solution. The alignment of second phases will influence the corrosion properties as well as the mechanical properties. Further work will concentrate on microscopy of fractured and corroded samples.

Corrosion

Given that corrosion behavior of Magnesium alloys depends strongly on electrolytes, this work was carried out using electrolyte other than the usual 3 % NaCl solution [1]. Ringer-Acetate solution is close to human blood and is more practical for bio-implantation materials compared to 3 % NaCl solution which is more aggressive. Although the influence of things like protein or serum content in the body may alter the corrosion behavior of the alloy under investigation, Ringer-Acetate solution is however useful for material screening. Figure 13 (a&b) shows selective development of corrosion on the surface of the sample in a Ringer-Acetate solution and (c) represents the fractured sample. Magnesium is usually anodic when in contact with most engineering materials in liquid environment [10]. As an alloy, the α-Mg matrix degrades preferentially due to the cathodic response of many precipitates [29]. The forms and distribution of the precipitates however play a role in determining the nature and dynamics of the corrosion. However, in this work, there is no very strong galvanic effect observed during corrosion apart from the selective attack as observed during the inception of the test as shown in figure 13 (a&b). This could be explained by the nature of the pH-value of the electrolyte which is mostly low (7-7.5) at the inception of the test and soon increases towards alkalinity (10.5) as the duration of the test increases. The increase in the pH-value lowers the rate of corrosion due to formation of $Mg(OH)_2$ which is stable at higher pH-values. Also the temperature has an influence on the corrosion rate; for evaluating OCP the corrosion rate is increased. Also the equilibrium potential is more positive at 37 °C and reaches saturation in shorter time, see figures 9 and 10. Previous work suggested that an accelerated corrosion of Magnesium alloy implant could be expected in vivo as the local pH was estimated at 7.4 or lower due to secondary acidosis resulting from metabolic and resorptive processes after surgery [5]. Another work shows that pH value (> 11.5) will promote a stable protective hydroxide layer on the surface of the Magnesium alloy implant while less than 11.5 will facilitate corrosion of the Magnesium alloy in corrosive media [30]. Zainal Abidin et al. [31] suggest corrosion tests in Hanks solution and to maintain the solution pH constant by CO_2 to avoid super-saturation. Furthermore it is mentioned, that increasing temperature increases the effect of microgalvanic corrosion followed by an increase of corrosion rate. Again, the microgalvanic reactions are not clear yet for the Mg10Gd system, but figures 11 and 12 show also increased corrosion rate. After strong corrosion leading into overlaid passivation and breakthrough the influence of temperature and microstructure is eliminated, because the corrosion rate seems to have reached its maximum, especially taking the ph-value increase into account.

Considering the Ringer-Acetate solution used in this work, extruded Mg10Gd shows a slightly more noble response (OCP) due to grain refinement compared to the as-cast material at 37 °C. However, it is planned to correlate each measured data with its local microstructure. As-cast material corrosion response will be influenced by the appearance of grain boundaries and dentritic arm spacing, wrought material has a more homogeneous microstructure (globular, fine grains), but aligned second phases which will promote microgalvanic corrosion, are distributed inhomogeneous. It is likely that the behavioral pattern may change in a different electrolyte as the alloying element reacts differently with respect to various corrosive media. However, bone implant materials are expected to corrode homogeneously while maintaining the necessary mechanical support needed within the healing duration [17].

Fatigue and corrosion fatigue

On the fatigue response of the investigated alloys, extruded Mg10Gd shows an increase in fatigue life over as-cast Mg10Gd in air as well as in Ringer-Acetate solution, even the fatigue strength itself has not been evaluated yet. As seen from the light microscopy images, strong grain refinement after recrystallization is the result of the extrusion process increasing the mechanical properties significantly.

From the fractured surface of as-cast Mg10Gd in figure 7 it is clear that the alloy exhibited a brittle transcrystalline fracture and one sees successive breaking of atomic bonds on the preferred crystallographic planes. The dominant slip systems in magnesium alloys are the basal {0001} <11-20>, prismatic {10-10} <11-20> and pyramidal {10-11} <11-20> systems including pyramidal twinning. At room temperature, plastic deformation occurs predominantly by basal slip and pyramidal twinning [28, 32]. The critical resolved shear stress (CRSS) for slip on {0001} basal planes and the prismatic {10-10} or pyramidal {10-11} planes differ considerably. Previous works [32, 33] show that the (CRSS) of either prismatic or pyramidal slip at 25 °C is several orders of magnitude higher than that of basal slip. This means that the probability of basal slip occurring even at grains unfavourably oriented for basal slip is high at room temperature. To have a complete picture of the fatigue and corrosion fatigue properties (particularly the fracture behavior), experiments should be repeated at 37 °C.

As observed from first microstructure images on as-cast Mg10Gd the grain boundaries alter the direction of crack propagation. Quasi crack blunting for finer grains (due to extrusion) was expected in comparison to coarse or columnar grain structures and could be as seen in this work. When the direction of the crack propagation lies on regions with more grain boundaries, the dislocation motion are delayed giving rise to longer fatigue life. In contrary, when the direction of crack propagation are purely transcrystalline as a result of coarse grains (as-cast condition), opposition to dislocation motion are greatly reduced giving rise to early fatigue failure as witnessed in [20]. The application of stress creates a plastic zone within the sample ahead of the crack tip: due

to columnar/ coarse grains, the critical stress to form twins is smaller. Again, boundaries between twins acts as strain build up regions [34]. Since the more driving force at this time is dislocation, crack follows up twin formation and the result for coarse alloys are mainly brittle fracture as observed in the investigated alloys. Reference [35] conducted fracture test on fine and coarse grain Mg-Zn-Al system and show that finer grains resist crack propagation better than coarse Magnesium alloy specimens. This is also true for fatigue tests as observed here for a Mg-Gd system, in as-cast and extruded condition. Finer grains will improve ductility thereby increasing the overall energy needed for crack initiation and propagation in the alloy. As shown in table I, the ultimate tensile strength for permanent mould chill cast Mg10Gd is 91 MPa respectively with ductility less than 2 %. This is very low compared to the standard stainless steel benchmark for stent purposes [7]. Application of grain size reduction due to appropriate manufacturing techniques has been seen to push these values higher (ultimate tensile strength of 251 MPa) and correspondingly improve the room temperature fatigue behavior of extruded Mg-Gd alloy system.

The selected corroded regions act as crack tip during fatigue test and thus strongly reduce the number of cycles to fracture in comparison to the fatigue test in air, in both as-cast and extruded condition. To evaluate the effect of the grain size or rather the number of grain boundaries, dendrite arms in the casting microstructure and the alignment of second phases in the extruded material further microscopic investigations are needed.

The interaction between the Ringer-Acetate solution and alloys lowers the overall fatigue strength of the alloys. However, in the as-cast material a uniform corroded surface was dictated after corrosion fatigue for 18 hours. Uniform corrosion is desirable as that will theoretically ensure the mechanical support of the implants reasonably before eventually degrading compared to strong pitting corrosion. Although most of the known Magnesium alloy precipitates have a more positive electrode potential than α-Mg matrix [29], the net distribution of the eutectic seems uniform on the permanent mould chill cast alloys investigated and as such the coarse segregated precipitates do not lead to strong galvanic situation causing pitting corrosion. For the extruded material no pitting corrosion in fatigue corrosion has been seen yet either, however, longer exposure times (by reducing the stress amplitude) need to be applied to get the overall picture.

From the work of Hort et al. [18, 36], when the Mg-Gd binary phase studied was heat treated to T4 and T6 conditions, its corrosion properties generally improved. For the as-cast Mg10Gd system, the T4 and T6 values were 0.7 mm/y and 0.4 mm/y respectively in 1 % NaCl solution [10, 18, 36]. This improved corrosion resistance was attributed to the nano scaled ß-precipitates which were uniformly distributed within the microstructure. It is well known that appropriate precipitates improve mechanical properties of Magnesium alloys. Heat treatment was not applied in this study, but recrystallization during extrusion also results in uniformly distributed precipitates, even showing some second phase alignment. Again, Peng et al. [37] reported an increase in corrosion resistance after a T4 treatment of GW103K which is a Mg-Gd-Y-Zr alloy in a 5 % NaCl. However, Birbilis and co-workers [38] show that increase in RE elements beyond a certain proportion will be detrimental to the corrosion properties of Magnesium alloys especially in as-cast condition. A combination of adequate alloying elements, Neodymium has already been discovered as an interesting candidate, heat treatment to encourage precipitates formation and uniform distribution will improve both the corrosion and fatigue properties of the Mg10Gd base alloying system.

Conclusion

Extruded Mg10Gd shows improved mechanical properties compared to the as-cast condition. This is mostly due to the grain refinement. Due to the CYS/TYS ratio above one, cyclic tensile creep occurs during fatigue tests predominantly, when the stress ratio is R=-1.

The improvement of the mechanical properties has no negative influence on the corrosion behavior. Extrusion of Mg10Gd show improved mechanical properties and fatigue strength both in air and in Ringer-Acetate solution.

Extruded Mg10Gd exhibited nobler characteristic (OCP) with respect to as-cast Mg10Gd at 37 °C, which is the environmental temperature for medical application. The improved properties observed in this extruded alloy are connected with the grain refinement. However, extended passivation during potentio-dynamic measurements has not been found. Corrosion rate at body temperature is found to be increased at potentials slightly higher than breakthrough potential. However, looking at the corrosion behavior at higher potentials, there is no difference between cast and wrought material and test temperature. Since the orientation of the exposed area for the potentiodynamic measurements is transversal to the extrusion direction (cross section), further tests on the longitudinal microstructure need to be done. Possible associated differences in behavior might occur.

Extruded Mg10Gd could be a potential implant material with further development; effort is however needed to produce more homogeneous and fine grained feedstock for wrought alloy production. Post casting processes such as heat treatments are sure ways of improving mechanical properties for biodegradable consumption.

Thermo-mechanical forming has shown first improvements. In-vivo experiments are necessary to gain more insight into Mg-Gd alloys. Also the influence of other rare earth elements on the Mg10Gd, for example Neodymium, is of interest. The increase of mechanical properties by alloying Neodymium to Mg10Gd in casting has already been proven in other studies.

Acknowledgement

The authors appreciate the support of Dipl.-Ing. Ralf Tesch in carrying out fatigue tests and Scanning Electron Microscopy. The assistance of Dipl.-Chem. Hartmut Habeck during corrosion tests, especially potentiodynamic measurements is greatly appreciated.

References

1. M.M. Avedesian and H. Baker, *Magnesium and Magnesium Alloys* (ASM Specialty Handbook 1999).
2. N. Winzer, A. Atrens, W. Dietzel, V.S. Raja, G. Song and K.U. Kainer, "Characterisation of stress corrosion cracking (SCC) of Mg-Al alloys," *Materials Science and Engineering: A*, 488 (1-2) (2008), 339-351.

3. G. Song, A. Atrens and M. Dargusch, "Influence of microstructure on the corrosion of die cast AZ91," *Corrosion Science*, 41 (2) (1998), 249-273.
4. O. Anopuo, N. Hort, Y. Huang and K.U. Kainer, "The influence of De-icing salts on corrosion of Mg-Alloys," *Magnesium Technology 2007*, ed. R.S. Beals, A.A. Luo, N.R. Neelameggham and M.O. Pekguleryuz, (2007), 439-444.
5. F. Witte, V. Kaese, H. Haferkamp, E. Switzer, A. Meyer-Lindenberg, C.J. Wirth and H. Windhagen, "In vivo corrosion of four magnesium alloys and the associated bone response," *Biomaterials*, 26 (17) (2005), 3557-3563.
6. L. Xu, G. Yu, E. Zhang, F. Pan and K. Yang, "In vivo corrosion behavior of Mg-Mn-Zn alloy for bone implant application," *Journal of Biomedical Research*, 83 (2007), 703-711.
7. H. Hermawan, D. Dubé and D. Mantovani, "Developments in metallic biodegradable stents," *Acta Biomaterialia*, 6 (2010), 1693-1697.
8. M. Peuster, P. Wohlsein, M. Brugmann, M. Ehlerding, K. Seidler and C. Fink, "A novel approach to temporary stenting: degradable cardiovascular stents produced from corrodible metal-results 6-18 months after implantation into New Zealand white rabbits," *Heart*, 86 (5) (2001), 563-569.
9. F. Witte, "The history of biodegradable magnesium implants: A review," *Acta Biomaterialia*, 6 (2010), 1680-1692.
10. A. Atrens, M. Liu and N.I.Z. Abidin, "Corrosion mechanism applicable to biodegradable magnesium implants," *Material Science and Engineering B*, 176 (20) (2011), 1609-1636.
11. H. Hermawan, A. Purnama, D. Dube, J. Couet and D. Mantovani, "Fe–Mn alloys for metallic biodegradable stents: Degradation and cell viability studies," *Acta Biomaterialia*, 6 (2010), 1852-1860.
12. M. Peuster, C. Hesse, T. Schloo, C. Fink, P. Beerbaum and C. Schnakenburg, "Long-term biocompatibility of a corrodible peripheral iron stent in the porcine descending aorta," *Biomaterials*, 27 (28) (2006), 4955-4962.
13. L. Xue, S. Dai and Z. Li, "Biodegradable shape-memory block co-polymers for fast self-expandable stents," *Biomaterials*, 31 (32) (2010), 8132-8140.
14. W.V.D. Giessen, C. Slager, H.V. Beusekom, D.V.I. Schenau, R. Huijts and J. Schuurbiers, "Development of a polymer endovascular prosthesis and its implantation in porcine arteries," *Journal of Interventional Cardiology*, 5 (3) (1992), 175-185.
15. G. Mani, M.D. Feldman, D. Patel and C.M. Agrawal, "Coronary stents: A materials perspective," *Biomaterials*, 28 (2007), 1689-1710.
16. C.J. McMahon, P. Oslizlok and K.P. Walsh, "Early restenosis following biodegradable stent implantation in an aortopulmonary collateral of a patient with pulmonary atresia and hypoplastic pulmonary arteries," *Catheterization and Cardiovascular Interventions*, 69 (2007), 735-738.
17. F. Witte, J. Fischer, J. Nellesen, H. Crostack, V. Kaese, A. Pisch, F. Beckmann and H. Windhagen, "In vitro and in vivo corrosion measurements of magnesium alloys," *Biomaterials*, 27 (2006), 1013-1018.
18. N. Hort, Y. Huang, D. Fechner, M. Störmer, C. Blawert, F. Witte, C. Vogt, H. Drücker, R. Willumeit, K.U. Kainer and F. Feyerabend, "Magnesium alloys as implant materials - Principles of property design for Mg-RE alloys," *Acta Biomaterialia*, 6 (2010), 1714-1725.
19. F.R. Elsayed, N. Hort, M.A. Salgado-Ordorica and K.U. Kainer, "Magnesium Permanent Mold Casting Optimization," *Materials Science Forum*, 690 (2011), 65-68.
20. P. Maier, O. Anopuo, F. Malchau, G. Wienck and N. Hort, "Cyclic deformation of newly developed Magnesium cast alloys in corrosive environment," *Materials Science Forum*, 690 (2011), 495-498.
21. A. Ball and B. Prangnell, "Tensile-compressive yield asymmetries in high strength wrought magnesium alloys," *Scripta Metallurgica of Materialia*, 31 (2) (1994), 111-116.
22. C. Fleck and D. Löhe, "Cyclic deformation behaviour of newly developed microalloyed Mg wrought alloys in corrosive environment," *Magnesium Technology 2007*, ed. R.S. Beals, A.A. Luo, N.R. Neelameggham and M.O. Pekguleryuz, (2007), 275-279.
23. P. Maier and C. Fleck, "Cyclic deformation of newly developed Magnesium wrought alloys microalloyed with Calcium in corrosive environment," (Paper presented at the Eurocorr 2007, The European Corrosion Congress: Progress by Corrosion Control 2007).
24. G. Lange, *Systematische Beurteilung technischer Schadens-fälle* (Wiley-VCH Weinheim 2001).
25. Pandat software package (PanMg7).
26. A.A. Nayeb-Hashemi, *Phase diagrams of binary magnesium alloys* (Metal Park, OH: ASM International, 1998).
27. J. Campbell, *Castings* (Oxford: Butterworth Heinemann, 2003).
28. E.F. Emley, *Principles of magnesium technology* (New York: Pergamon Press, 1966).
29. O. Lunder, K. Nisancioglu and R.S. Hanses, "Corrosion of Die Cast Magnesium-Aluminum Alloys," *SAE Technical Paper*, (1993), 930755.
30. M. Pourbaix, *Atlas of Electrochemical equilibria in aqueous solutions* (National Association of Corrosion Engineers, Houston, 1974).
31. N.I. Zainal Abidin, A.D. Atrens, D. Martin and A. Atrens, "Corrosion of high purity Mg, Mg2Zn0.2Mn, ZE41 and AZ91 in Hank's solution at 37 °C," *Corrosion Science*, 53 (2011), 3542-3556
32. P. B. Hirsch and J. S. Lally, "Deformation of magnesium single crystals," *Philosophy Magazine*, 12 (1965), 595-648.
32. P. W. Bakarian and C. H. Matthewson, "Slip and twinning in magnesium single crystals at elevated temperature," *Transactions of the Metallurgical Society of AIME*, 152 (1943), 226-254.
33. B. C. Wonsiewicz and W. A. Backofen, "Plasticity of magnesium crystals," *Transactions of the Metallurgical Society of AIME*, 239 (1967), 1422-1431.
34. H. Somekawa, A. Singh and T. Mukai, "Fracture mechanism of a coarse grained magnesium alloy during fracture toughness testing," *Philosophical Magazine Letters*, 89 (2009), 2-10.
35. H. Somekawa, A. Singh and T. Mukai, "Fracture mechanism and toughness in fine and coarse grained magnesium alloys," *Magnesium Technology 2011*, ed. W.H. Sillekens, S.R. Agnew, N.R. Neelameggham and S.N. Mathaudhu, (2011), 25-28.
36. K.U. Kainer, N. Hort, R. Willumeit, F. Feyerabend and F. Witte, *Processing of Advanced Materials 18*, ed. M. Niinomi, M. Morinaga, M. Nakai, N. Bhatnagar and T.S. Srivatsan, (2009), 975-984.
37. L.M. Peng, J.W. Chang, X.W. Guo, A. Atrens, W.J. Ding and Y.H. Peng, "Influence of heat treatment and microstructure on the corrosion of magnesium alloy Mg-10Gd-3Y-0.4Zr," *Journal of Applied electrochemistry*, 39 (2009), 913-920.
38. N. Birbilis, M.A. Easton, A.D. Sudholz, S.M. Zhu and M.A. Gibson, "On the corrosion of binary magnesium - rare earth alloys," *Corrosion Science*, 51 (2009), 683-689.